Silica-supported zirconocene/(perfluorophenyl)borate catalyst for propylene polymerization
DRIFTS study of the catalyst formation and surface species

V.N. Panchenko*, I.G. Danilova, V.A. Zakharov, E.A. Paukshtis

Boreskov Institute of Catalysis, Siberian Branch of Russian Academy of Sciences, Prospect Akademika Lavrentieva, 5, Novosibirsk 630090, Russia

Abstract

IR spectroscopy has been used to study the interaction of silica with $PhNEt_2$ (N) and $B(C_6F_5)_3$ (B) and subsequent interaction of the support $SiO_2/[N + B]$ with dimethylzirconocene $Me_2Si(2\text{-}Me\text{-}Ind)_2ZrMe_2$ ("Zr"). The data were obtained on the composition of the surface compounds appeared at both stages of catalyst synthesis.

It has been shown that (B) and (N) interact with OH groups of silica to form ionic pair $[H-NR_3]^+[(C_6F_5)_3B-O-Si\equiv]^-$ (IP-1). Cation fragment of this pair contains highly reactive N—H bond with a.b. at $3230\,cm^{-1}$. It has been found that N—H groups in a part of IP-1 complexes react with neighboring OH groups of silica by hydrogen bonding that gives complexes IP-2. It has been shown that "Zr" complexes interact both with complexes IP-1 and IP-2. As "Zr" reacts with IP-1, zirconium ionic complexes IP-3 containing Zr—Me bond are formed on silica. These complexes are suggested to be the precursor of the polymerization active sites. The reaction of "Zr" with IP-2, most likely, produces surface zirconium compound containing no Zr—Me bonds and inactive for propylene polymerization.
© 2004 Elsevier B.V. All rights reserved.

Keywords: FTIRS; Supported zirconocene catalysts; Perfluoroarylborate activator; Propylene polymerization

1. Introduction

Metallocenes when used in combination with suitable activating agents (polymethylalumoxane (MAO) or perfluoroarylborate activators (FAB)) are extremely active catalysts for alkene polymerization [1,2]. The studies of homogeneous metallocene systems proved that dimethyl zirconocene derivatives react with MAO or FAB to produce ionic pairs of composition ($[Cp_2ZrMe]^+[B(C_6F_5)_4]^-$ or $[Cp_2ZrMe]^+[Me\text{-}MAO]^-$) [3–6], which are assumed to be the precursors of the active sites at polymerization.

Supported metallocene catalysts are considered the most promising for practical applications. Common approach to synthesize these catalysts consists in supporting metallocene complexes on silica modified with MAO [7–9].

One of the methods to synthesize of MAO-free supported metallocene catalysts has been patented by Exxon Chem. Co. [10]. According to this patent and Refs. [11–15,24,25], supported ionic pairs are formed at the treatment of silica with alkyl aniline and *tris*-pentafluorophenyl boron followed by supporting of dimethylzirconocene (Scheme 1).

The composition and structure of surface species $[HNR_3]^+[(C_6F_5)_3BOSi\equiv]^-$ has been investigated by IR and multinuclear solid-state NMR spectroscopies [24]. It has been shown that the unique $[HNR_3]^+[(C_6F_5)_3BOSi\equiv]^-$ fragments are formed at highly dehydroxylated silica, whereas two sorts of surface sites: free silanol groups and ionic species $[HNR_3]^+[(C_6F_5)_3BOSi\equiv]^-$ are formed at lower dehydroxylated silica.

IRS and solid-state CP-MAS ^{13}C NMR studies [25] confirm that zirconocene (Cp^*ZrMe_3) reacts primarily with the surface anilinium cation as it shown in Scheme 1.

* Corresponding author. Fax: +7 3832 344687.
E-mail address: panchenko@catalysis.nsk.su (V.N. Panchenko).
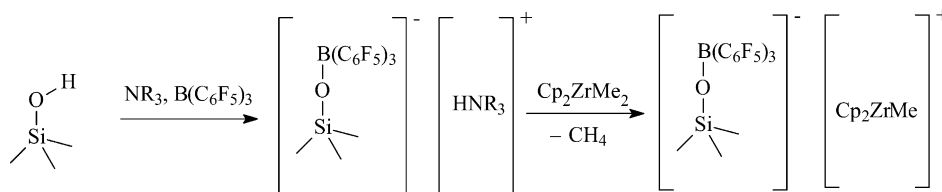
Scheme 1. Proposed scheme of MAO-free supported catalyst [10,11].

In the present work, we have used FTIRS in diffuse reflection (DRIFT) modes in more detail to study the reaction of silica with $PhNEt_2$ and $B(C_6F_5)_3$ and subsequent reaction of the support obtained with dimethylzirconocene $Me_2Si(2\text{-}Me\text{-}Ind)_2ZrMe_2$. DRIFTS is very effective method for study of real catalyst samples in powder form. In this case, the same catalyst samples are used both for polymerization and study of the surface species by DRIFTS. So it is more reliable way to consider the correlation between data on the surface species and activity at polymerization and analyze the effect of preparation details on the surface species and activity. We have studied the composition of the surface compounds formed at both stages of catalyst formation by means of DRIFTS mainly. The data on the catalyst performance in propylene polymerization are presented as well.

2. Experimental

The experiments were performed using the "break seal" technique.

$Me_2Si(2\text{-}Me\text{-}Ind)_2ZrMe_2$, $PhNEt_2$, $B(C_6F_5)_3$ and SiO_2 (MS Davison 952, specific surface area $310\,m^2/g$, pore volume $1.8\,cm^3/g$) were donated by Exxon-Mobil.

2.1. Synthesis of support

The measured sample of silica was heated in air at $500\,°C$ for 3 h, then placed into a quartz ampoule and dehydroxylated in vacuum at $800\,°C$ for 3 h. In some case, silica was dehydroxylated in vacuum at 400 or $600\,°C$ for 3 h.

$SiO_2/B(C_6F_5)_3$ and $SiO_2/PhNEt_2$ samples have been prepared by treating of silica with toluene solutions of $B(C_6F_5)_3$ (molar ratio of B:OH = 1.2) and $PhNEt_2$ (molar ratio of N:OH = 1.2), respectively. The suspension was agitated for 1 h at room temperature and then washed out with toluene and dried in vacuum.

$SiO_2/[PhNEt_2/B(C_6F_5)_3]$ sample has been synthesized as following. Silica was treated with toluene solution of $PhNEt_2$ (molar ratio of N:OH = 1.2) at room temperature. The suspension was agitated for 1 h, then $B(C_6F_5)_3$ was added to adjust B:OH = 1.2. The suspension was agitated for 1 h, then washed out with toluene four times and dried in vacuum at room temperature.

2.2. Synthesis of catalyst

Support $SiO_2/[NEt_2Ph/B(C_6F_5)_3]$ was treated with toluene solution of zirconocene $Me_2Si(2\text{-}Me\text{-}Ind)_2ZrMe_2$ adjusting molar ratios of Zr:OH = 1.25, 0.7 and 0.4 at room temperature. The suspension was agitated for 0.5 h, the catalyst was washed out with toluene four times and dried in vacuum at room temperature.

2.3. Studies of chemical composition of supports and catalysts

2.3.1. DRIFT study

The samples of supports and catalysts in a form of dry powders were placed into a special cell for DRIFT measurements under vacuum. The DRIFT spectra are presented in a form of Kubelka-Munk function [16]:

$$F(R) = \frac{(1 - R)^2}{2R} \tag{1}$$

where R is the reflection coefficient.

The DRIFT spectra were recorded on a Shimadzu FTIR-8300 spectrometer with DRS-8000 diffusion attachment in the 400–$6000\,cm^{-1}$ range with a resolution of $4\,cm^{-1}$.

2.3.2. IRS study (transmission mode)

The silica powder was pressed into tablets (mass typically $\rho = 10$–$15\,mg/cm^2$). The silica tablet was heated in air at $500\,°C$ for 1 h, then placed in a special cell and dehydroxylated at $800\,°C$ for 1 h at a pressure below 2×10^{-2} Torr. Dehydroxylated sample was cooled to room temperature and treated as described below. The samples of $SiO_2/B(C_6F_5)_3$ and $SiO_2/PhNEt_2$ were produced by treating of silica tablets with toluene solutions of $B(C_6F_5)_3$ (molar ratio of B:OH = 40) and $PhNEt_2$ (molar ratio of N:OH = 40), respectively.

The sample of $SiO_2/[PhNEt_2/B(C_6F_5)_3]$ was prepared as follows. The silica tablet was treated with toluene solution of NEt_2Ph (N:OH = 40) for 30 min, then the toluene solution of $B(C_6F_5)_3$ (B:OH = 40) was added. After 30 min the solution was decanted and the tablet washed out with toluene three times and dried under vacuum. Then the IRS measurements were performed.

The sample SiO_2/BCl_3 has been prepared by treatment of silica with BCl_3 (0.4 atm BCl_3) into the cell. The tablet was kept in BCl_3 at $400\,°C$ for 0.5 h, then the cell was vacuumed

to $2 \cdot \times 10^{-2}$ Torr at 400 °C. Then the treatment of the sample by BCl_3 was repeated.

The IR spectra were recorded on a Shimadzu FTIR-8300 spectrometer in the 400–6000 cm^{-1} range with a resolution of 4 cm^{-1}.

2.4. Studies of chemical composition

The content of aluminium and boron in the samples have been determined by means of inductively coupled plasma-atomic emission spectrometry (ICP-AES) as described in [17].

2.5. Polymerization

The catalysts were tested in propene slurry polymerization in a steel autoclave (1.0 L) under the following conditions: catalyst loading 0.03–1 g, heptane (250 mL), temperature 70 °C, propene pressure 4 bar, co-catalyst $Al(i-Bu)_3$ (0.72 mmol/L), 2 vol.% of H_2, polymerization for 30 min.

3. Results and discussion

3.1. The study of silica interaction with $B(C_6F_5)_3$ and NEt_2Ph

First we have studied the interaction of silica dehydroxylated at 800 °C with individual FAB components (($B(C_6F_5)_3$ and $PhNEt_2$). Fig. 1 presents the DRIFT spectra of $SiO_2/B(C_6F_5)_3$ and $SiO_2/PhNEt_2$ samples.

Small decrease of intensity of a.b. at 3745 cm^{-1} (terminal Si–OH groups) and appearance of the broad a.b. at 3720 and 3640 cm^{-1} are observed after treatment of silica with $B(C_6F_5)_3$ (Fig. 1, spectra 1 and 2). These new bands are attributed to hydrogen-bonded OH groups resulting from the reaction of terminal Si–OH groups with fluoroaryl groups in $B(C_6F_5)_3$. Besides, the DRIFT spectrum of $SiO_2/B(C_6F_5)_3$ sample contains a set of a.b. at 3100–2700 cm^{-1} range, originating from stretching vibrations of C–H of toluene used as a solvent. According to the data of chemical analysis (Table 1), boron content in $SiO_2/B(C_6F_5)_3$ is very low (0.07 wt.%) that agreed with insignificant decrease of intensity of the a.b. at 3745 cm^{-1}. The chemical analysis and DRIFTS data allow suggestion that $B(C_6F_5)_3$ is fixed on the support surface owing to hydrogen bonding of Si–OH and fluoroaryl groups.
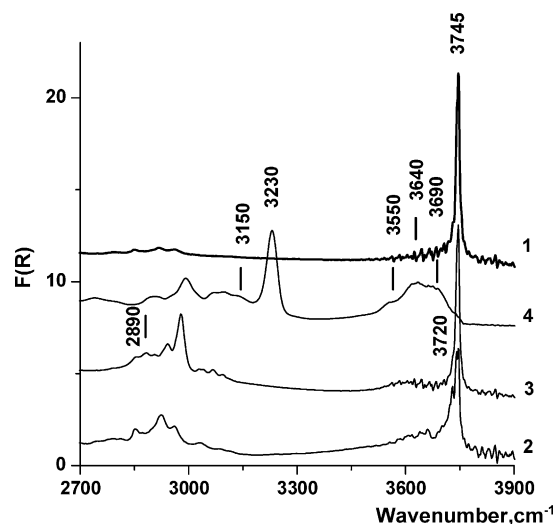
Fig. 1. DRIFT spectra of (1) $SiO_2(800)$, (2) $SiO_2(800)/B(C_6F_5)_3$, (3) $SiO_2(800)/Et_2NPh$ and (4) $SiO_2(800)/Et_2NPh/B(C_6F_5)_3$.

The intensity of a.b. at 3745 cm^{-1} also slightly decreases after treatment of silica with $PhNEt_2$ (Fig. 1, spectra 1 and 3). Broad and little intensive a.b. with a maximum at 3640 cm^{-1} (hydrogen-bonded Si–OH groups) are appeared. Besides, the spectrum displays a set of a.b. at 2700–3100 cm^{-1} range, characteristic for C–H stretching vibrations in Et and Ph groups and toluene molecules. These results suggest that $PhNEt_2$ adsorbed on silica fails to react efficiently with terminal OH groups. Only insignificant part of OH groups forms surface compounds due to hydrogen bonding. However, even low-efficient reaction of NEt_2Ph with OH groups seems to weaken the SiO–H bond and thus facilitate subsequent reaction of silanol group with borate.

After successive treatment of silica with $PhNEt_2$ and $B(C_6F_5)_3$ the a.b. at 3745 cm^{-1} disappears while new a.b. at 2800–3100, 3150, 3230, 3550, 3640 and 3690 cm^{-1} appear (Fig. 1, spectrum 4). a.b. at 2800–3100 cm^{-1} can be attributed to the stretching vibrations of C–H bonds in organic molecules. a.b. at 3500–3730 cm^{-1} are characteristic for stretching vibrations of hydrogen-bonded Si–OH groups originated from the reaction of terminal OH groups with the adsorbed molecules.

The presence of a.b. at 3150 and 3230 cm^{-1} in the spectrum of $SiO_2/[PhNEt_2/B(C_6F_5)_3]$ is of key importance in the context of the present study. According to Refs. [20–22,24], these bands can be attributed to N–H stretching vibrations

Table 1
Data on boron content in the samples SiO_2/X

No.	X	B (μmol/g) (wt.%)	[OH]/[B]	Zr μmol/g (wt.%)	[OH][a]/[Zr]	[Zr]/[B]
1	BCl_3	364 (0.4)	1.04	–	–	–
2	$B(C_6F_5)_3$	63.6 (0.07)	5.98	–	–	–
3	$PhNEt_2 + B(C_6F_5)_3$	210 (0.23)	1.8	–	–	–
4	$PhNEt_2 + B(C_6F_5)_3 + Zr$	210 (0.23)	1.8	198 (1.8)	1.92	0.94

[a] OH groups content in initial silica calculated according to IRS data is 380 μmol/g [18].

in a surface species formed at interaction of Si–OH groups with PhNEt$_2$ and B(C$_6$F$_5$)$_3$. a.b. at 3230 cm^{-1} is specific for the stretching vibrations of unperturbed N–H bond in a surface complex [H-NR$_3$]$^+$[A]$^-$. The appearance of a.b. at 3230 cm^{-1} in IR spectra was observed after treatment of silica with PhNEt$_2$ and B(C$_6$F$_5$)$_3$ in [24]. Data presented in [24] and our data (Fig. 1) evidence clearly on the formation of ionic pair (IP-1) via reaction (2):

≡Si–OH + Et$_2$NPh + B(C$_6$F$_5$)$_3$

$$\rightarrow \underset{\text{(IP-1)}}{[\equiv\text{Si–O–B(C}_6\text{F}_5)_3]^- [\text{H–NEt}_2\text{Ph}]^+} \tag{2}$$

A.b. at 3150 cm^{-1} most likely originates from stretching vibrations of N–H bond from [H-NR$_3$]$^+$, that is hydrogen-bonded to silica OH group (≡N–H...O(H)–Si≡) (IP-2, reaction (3)). Then a.b. at 3550 cm^{-1} can be attributed to OH stretching vibrations in IP-2:

$$\begin{array}{l} \equiv\!\!\equiv\!\text{Si–OH} \quad + \quad \text{Et}_2\text{NPh} \quad + \quad \text{B(C}_6\text{F}_5)_3 \\ \equiv\!\!\equiv\!\text{Si–OH} \end{array} \tag{3}$$

$$\longrightarrow \left[\equiv\!\!\equiv\!\text{Si–O–B(C}_6\text{F}_5)_3\right]^- \left[\begin{array}{c} \text{H–NEt}_2\text{Ph} \\ \uparrow \qquad \downarrow \\ \equiv\!\!\equiv\!\text{Si–O–H} \end{array}\right]^+$$

(IP-2)

The data on the boron content in SiO$_2$/[PhNEt$_2$/B(C$_6$F$_5$)$_3$] sample confirm this suggestion (Table 1). Indeed, successive treatment of silica with PhNEt$_2$ and B(C$_6$F$_5$)$_3$ results in a sharp increase of boron content in support (0.23 wt.%) as compared with SiO$_2$/B(C$_6$F$_5$)$_3$ sample (0.07 wt.%). However, the concentration of the bounded boron is lower than the content of terminal OH groups (210 and 380 μmol/g, respectively). This observation is consistent with the data on high content of hydrogen-bonded OH groups that display the broad a.b. at 3550–3700 cm^{-1}.

The sequence of reagents supporting on silica is of no importance. Supports SiO$_2$/[PhNEt$_2$ + B(C$_6$F$_5$)$_3$] and SiO$_2$/[B(C$_6$F$_5$)$_3$ + PhNEt$_2$] showed similar boron contents (0.23 and 0.21 wt.%, respectively) and similar DRIFT spectra.

Earlier it has been shown that [24], the unique ionic pairs (IP-1) are formed at highly dehydroxylated silica, while two kinds of surface sites: free silanol groups and ionic pairs (IP-1) are formed at lower dehydroxylated silica. The percentage of boron corresponds to a proportion of modified OH groups increases with increasing silica dehydroxylation temperature [24]. So it is interesting to get data on the effect of dehydroxylation temperature of silica on the formation of ionic pairs (IP-1) and (IP-2).

DRIFT spectra of the samples SiO$_2$/[NEt$_2$Ph/B(C$_6$F$_5$)$_3$] prepared using silica dehydroxylated at 400, 600, 800 °C are presented in Fig. 2. DRIFT spectra of all samples contain the similar a.b. at 3230 cm^{-1} from the surface compound (IP-1)

Fig. 2. Different DRIFT spectra of samples SiO$_2$(Td)/NEt$_2$Ph/B(C$_6$F$_5$)$_3$ dehydroxylation temperature of silica: (1) 400 °C, (2) 600 °C and (3) 800 °C.

and a.b. at 3150 and 3550 cm^{-1} from the surface compound (IP-2). The intensity of a.b. at 3230 cm^{-1} changes insignificantly with growth of silica dehydroxylation temperature. The intensity of a.b. at 3150 and 3550 cm^{-1} increases with decreasing silica dehydroxylation temperature.

Data of chemical composition of the samples are given in Table 2. The total content of silica OH groups noticeably reduced whereas the amount of terminal OH groups changes insignificantly with increasing silica dehydroxylation. Boron content slightly decreases with the increase of silica dehydroxylation temperature. Not all OH groups interact with boron activator. The ratio [B]/[Σ-OH] groups grows from 0.28 to 0.56 with increase of silica dehydroxylation temperature from 400 to 800 °C, at the same time the ratio [B]/[terminal-OH] slightly decreases from 0.69 to 0.56. According to the results obtained, the borate activator interacts mainly with terminal OH groups of silica.

The surface compounds (IP-1) and (IP-2) contain the bonds ≡Si–O–B in the structures [≡Si–O–B(C$_6$F$_5$)$_3$]$^-$ (A$^-$). We studied the formation of ≡Si–O–B bond in the structures (A$^-$) by means of FTIRS (transmission modes). The samples SiO$_2$/PhNEt$_2$/B(C$_6$F$_5$)$_3$ and SiO$_2$/BCl$_3$ have been prepared for this study by treatment of silica tablets with (i) PhNEt$_2$ and then B(C$_6$F$_5$)$_3$; (ii) BCl$_3$ directly in the IRS cell for FTIRS measurements (see Section 2). The IR spectra of these samples are shown in Fig. 3.

The IR spectrum of SiO$_2$/BCl$_3$ sample shows only the broad asymmetrical band with two maxima at 1380 and 1410 cm^{-1} (Fig. 3, spectrum 1). According to Refs. [19,20], these bands are attributed to B–O stretching vibrations in (≡SiO)BCl$_2$ (1380 cm^{-1}) and (≡SiO)$_2$BCl (1410 cm^{-1}). The a.b. at 3745 cm^{-1} (terminal Si–OH groups) is absent in the spectrum of this sample.

Table 2
Data on composition of $SiO_2(Td)/[N + B]$ samples

No.	Td^a	$[\Sigma\text{-OH}]^b$ (μmol/g)	$[t\text{-OH}]^c$ (μmol/g)	[B] (wt.%) (μmol/g)	$[B]/[\Sigma\text{-OH}]$	$[B]/[t\text{-OH}]$
1	400	961	391	0.3 (272)	0.28	0.69
2	600	530	380	0.27 (246)	0.46	0.64
3	800	376	376	0.23 (209)	0.56	0.56

[a] Dehydroxylation temperature of silica (°C).

[b] $[\Sigma\text{-OH}]$: terminal and hydrogen-bonded OH groups ($3745 - 3680\,\text{cm}^{-1}$) content in initial silica calculated according to IRS data [18].

[c] $[t\text{-OH}]$: terminal OH groups ($3745\,\text{cm}^{-1}$) content.

SiO_2/BCl_3 sample contains 0.44 wt.% of B (364 μmol/g, Table 1). Molar ratio [OH]/[B] = 0.98 means that BCl_3 reacts almost quantitatively with Si−OH groups (reaction (4)).

$$\equiv\text{Si−OH} + BCl_3 \rightarrow \equiv\text{Si−O−}BCl_2 + HCl \qquad (4)$$

Also the intensive a.b. at $1370–1410\,\text{cm}^{-1}$ region is observe in the spectrum of $SiO_2/PhNEt_2/B(C_6F_5)_3$ sample (Fig. 3, spectrum 2). But a.b. bending vibrations from C−H stretches of NEt_2Ph are present in the same frequency region. So the separation of Si−O−B bond in $SiO_2/PhNEt_2/B(C_6F_5)_3$ sample is quite problematic.

Thus, our data show that successive treatment of silica with $B(C_6F_5)_3$ and $PhNEt_2$ caused the reaction of terminal OH groups from silica with these compounds resulted in the formation of ionic pair (IP-1). Cation fragment of (IP-1) contains highly reactive N−H bond. This fragment can be involved in a side reaction with silica OH groups by hydrogen bonding that gives complex (IP-2) (reaction (3)).

3.2. The study of metallocene $Me_2Si(2\text{-}Me\text{-}Ind)_2ZrMe_2$ ("Zr") interaction with support $SiO_2/[PhNEt_2/B(C_6F_5)_3]$ ($SiO_2/[N + B]$)

The DRIFT spectra of support $SiO_2/[N + B]$ and catalyst $SiO_2/[N + B]/$"Zr" are shown in Fig. 4.

It is seen that a.b. $3230\,\text{cm}^{-1}$ decreases sharply at interaction of zirconocene with support $SiO_2/[N + B]$ (Fig. 3). That means that zirconocene reacts with the surface complex IP-1 via reaction (5) that likely leads to the formation of the surface zirconium complex (IP-3).

$$[\equiv\text{Si−O−}B(C_6F_5)_3]^-[\text{H−}NEt_2Ph]^+ \xrightarrow[-PhNEt_2,\ CH_4]{+RL_2ZrMe_2}$$
$$(\text{IP-1})$$
$$[\equiv\text{Si−O−}B(C_6F_5)_3]^-[RL_2ZrMe]^+ \qquad (5)$$
$$(\text{IP-3})$$

It should be noted that the disappearance of the ν(NH) vibration at $3230\,\text{cm}^{-1}$ initially presented in the spectrum of $SiO_2/[NEt_2Ph/B(C_6F_5)_3]$ support was observed after adsorption of Cp^*ZrMe_3 in [25]. It has been shown by solid-state ^{11}B NMR spectroscopy that the surface anion $[=SiOB(C_6F_5)_3]^-$ is present after reaction of zirconocene with support.

Intensities of a.b. at 3150 and $3550–3700\,\text{cm}^{-1}$ in the catalyst spectrum are also lower than in the support spectrum. This observation may be attributed to the reaction of zirconocene with surface compound (IP-2) via reaction (6). This reaction results to the formation of surface zirconium complex (IP-4) that contains no Zr−Me bonds.

Fig. 3. DRIFT spectra of (1) $SiO_2(800)/BCl_3$ and (2) $SiO_2(800)/NEt_2Ph/B(C_6F_5)_3$.

Fig. 4. DRIFT spectra of (1) $SiO_2/PhNEt_2/B(C_6F_5)_3$ and (2) $SiO_2/PhNEt_2/B(C_6F_5)_3/Me_2Si(2\text{-Me-Ind})_2ZrMe_2$ (zirconium content 1.8 wt.%).

$$\left[\equiv\!\!\mathrm{Si-O-B(C_6F_5)_3}\right]^-\left[\begin{array}{c}\mathrm{H-NEt_2Ph}\\ \equiv\!\!\mathrm{Si-O-H}\end{array}\right]^+ \xrightarrow[\mathrm{-PhNEt_2,\ CH_4}]{\mathrm{+\ RL_2ZrMe_2}} \left[\equiv\!\!\mathrm{Si-O-B(C_6F_5)_3}\right]^-\left[\begin{array}{c}\mathrm{RL_2Zr}\\ \equiv\!\!\mathrm{Si-O}\end{array}\right]^+ \tag{6}$$

$$\text{(IP-2)} \qquad\qquad\qquad\qquad \text{(IP-4)}$$

We cannot exclude the reaction between hydrogen-bonded Si–OH groups and zirconocene complex with formation of inactive μ-oxo-zirconium compounds. But this reaction is probably insignificant because the intensity of a.b. at 3630 and 3700 cm^{-1} slightly decreases. Most part of SiOH groups is inaccessible for zirconocene due to steric hindrance of the bulky supported boron activator.

Table 1 shows the data on the chemical composition for the support SiO$_2$/[N + B] and catalyst SiO$_2$/[N + B]/"Zr". It is seen that boron content in the support and catalyst is the same. That means that FAB in (IP-1) and (IP-2) surface species is tightly bound to silica surface. Molar ratio of Zr/B in catalyst SiO$_2$/[N + B]/"Zr" is close to unit (Zr/B = 0.94). Thus, the data of chemical analysis are consistent with the DRIFT results and reactions (5) and (6).

The above results were obtained at the studies of catalysts prepared by supporting of excessive amount of zirconocene (Zr/B = 1.96). We have studied the SiO$_2$/[N+B]/"Zr" samples synthesized at different Zr/B ratios.

Fig. 5 presents the DRIFT spectra of the catalysts prepared by supporting of different amount of "Zr" on SiO$_2$/[N + B] support. It is seen that after treatment of support with "Zr" at ratio Zr$_{in}$/B = 0.53, the intensities of a.b. at 3150 and 3550 cm^{-1} decrease considerably, while intensity of a.b. 3230 cm^{-1} (ν_{N-H}) remains almost the same (Fig. 5, spectra 1 and 2). As the ratio Zr$_{in}$/B increases, the intensities of a.b. at 3230 cm^{-1} decreases (Fig. 5, spectra 3 and 4).
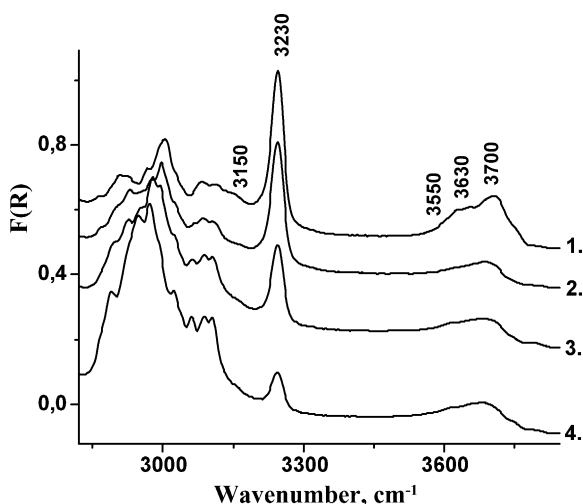
Fig. 5. DRIFT spectra of (1) support SiO$_2$/PhNEt$_2$/B(C$_6$F$_5$)$_3$, (2–4) catalysts SiO$_2$/PhNEt$_2$/B(C$_6$F$_5$)$_3$/Me$_2$Si(2-Me-Ind)$_2$ZrMe$_2$: (2) 0.47% wt. Zr, Zr$_{in}$/B = 0.53, (3) 1.16 wt.% Zr, Zr$_{in}$/B = 1.26, (4) 1.8 wt.% Zr, Zr$_{in}$/B = 1.96 (Zr$_{in}$ – initial amount of zirconocene used for catalyst preparation).

Thus the DRIFT data allow suggest that as "Zr" is supported on SiO$_2$/[N + B] support, it reacts first with the surface complexes (IP-2) by reaction (6); if in excess Zr reacts with surface complexes (IP-1) via reaction (5).

The data on the chemical composition of the catalysts with different of zirconium content are listed in Table 3. It is seen that zirconium content in the catalysts was almost twice lower than zirconium loading. Even in sample 3 which was prepared by supporting twice lower amount of zirconocene with respect to boron content in the support (Zr$_{in}$/B = 0.53) only a half of loaded zirconocene was detected in the catalyst. Most likely a part of zirconocene was involved into side reactions accompanying catalyst synthesis in particular into reaction with an amine released during reactions (5) and (6). This side reaction seems to produce soluble zirconocene–amine complex removed by catalyst washings.

Only the use of excess of zirconocene (Table 3, exp. 1, Zr$_{in}$/B = 1.96) allows reaction of practically all (IP-1) complexes with zirconocene (Zr/B = 0.94 in respective catalyst).

3.3. Catalytic properties of SiO$_2$/[N+B]/"Zr" catalysts in propylene polymerization

Data on the activity of SiO$_2$/[N+B]/"Zr" catalysts differing by zirconocene in propylene polymerization are presented in Table 3. Obviously activity correlates with zirconium content in the catalyst. The catalyst with the highest zirconium content (Zr$_C$/B = 0.94) showed the maximal activity. Thus, as zirconocene reacts with SiO$_2$/[N + B] first reaction (6) proceeds to form surface species which are inactive for propylene polymerization, and then surface species active for propylene polymerization are formed by reaction (5).

The data on the activity of catalysts differed by zirconium content are consistent with respective DRIFT data discussed above (Fig. 5).

Fig. 6 illustrates the kinetics of propylene polymerization with catalyst No. 1 from Table 3. The polymerization reaction was unsteady state (decay type). The maximal activity is observed for the first 5 min on-stream; then the catalyst deactivated rapidly. Meanwhile the nature of catalyst deactivation remains unclear.

Hydrogen input into reaction mixture increases greatly the initial activity but kinetic profile is decay type too (Fig. 6, curve 2). The effect of activation of propylene polymerization with zirconocene catalysts in hydrogen presence was observed in a number of researches [22,23].

Table 3
Data on the composition and activity of catalysts SiO_2/[N + B]/Zr in propylene polymerization

No.	Initial content of Zr		Catalyst composition			Yield[b] (g_{PP}/g_{cat})	Activity[c] (kg_{PP}/g_{Zr} min)
	Zr_{in} (μmol/g)	Zr_{in}/B^a (mol/mol)	Zr (μmol/g)	Zr/B (mol/mol)	Zr/Zr_I (mol/mol)		
1	470	1.96	198	0.94	0.42	400	57.4
2	263	1.26	127	0.61	0.48	268	23
3	110	0.53	52	0.25	0.48	10	2.2

Boron support content is 0.23 wt.%.

[a] Content of boron in the support is 0.23 wt.%.
[b] Yield of PP for 30 min.
[c] Initial activity for the first 5 min.
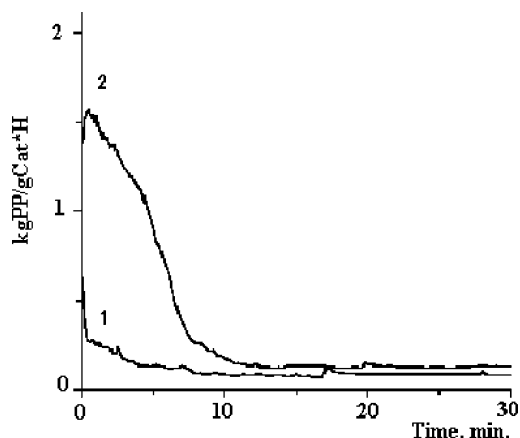
Fig. 6. The kinetic profile of catalyst SiO_2/[N + B]/Zr in propylene polymerization at 70 °C, propylene pressure 4 bar, with $Al(i\text{-}C_4H_9)_3$ as scavenger: (1) polymerization without H_2 and (2) polymerization with H_2 (2 vol.% of H_2).

References

[1] T.J. Marks, Accounts Chem. Res. 25 (2) (1992) 57–65.
[2] W. Kaminsky, Macromol. Chem. Phys. 197 (1996) 3907–3945.
[3] M. Bochmann, J. Chem. Soc., Dalton Trans. 3 (1996) 255.
[4] R.F. Jordan, Adv. Organomet. Chem. 32 (1991) 325.
[5] E.Y.X. Chen, T.J. Marks, Chem. Rev. 100 (2000) 1391–1434.
[6] D.E. Babushkin, N.V. Semikolenova, V.A. Zakharov, E.P. Talsi, Macromol. Chem. Phys. 207 (2000) 558–567.
[7] W. Kaminsky, A. Laban, Appl. Catal. A: Gen. 222 (2001) 47–61.
[8] E.M. Carnahan, G.B. Jacobsen, Catal. Technol. 4 (1) (2000) 74–88.
[9] E. Wasserman, Metallocenes, in: I.T. Horvath (Ed.), Encyclopedia of Catalysis, vol. 4, John Wiley and Sons, Inc., New Jersey, 2003, pp. 725–789.
[10] J.F. Walzer Jr., Supported ionic catalyst composition, Exxon Chemical Co. US Patent 5,643,847 (1997).
[11] G.G. Hlatky, D.J. Upton, Macromolecules 29 (1996) 8019–8020.
[12] J. Lancaster, S.M. O'Hara, M. Bochmann, in: W. Kaminsky (Ed.), Metalorganic Catalysts for Synthesis and Polymerization, Springer-Verlag, Berlin, 1999, pp. 413–425.
[13] S.B. Roscoe, J.M.J. Frechet, J.F. Walzer, A.J. Dias, Science 280 (10) (1998) 270–273.
[14] H.C.L. Abbenhuis, Angew. Chem. Int. Ed. 38 (8) (1999) 1058–1060.
[15] S. Charoenchaidet, S. Chavadej, E. Gulari, J. Polym. Sci. A: Polym. Chem. 40 (2002) 3240–3248.
[16] L.M. Kustov, Top. Catal. 4 (1997) 131.
[17] M. Thompson, J.N. Walsh, A Handbook of Inductively Coupled Plasma Spectrometry, Blakie and Son.- Bishopbriggs, Glasgow, England, 1983.
[18] A.V. Kiselev, V.I. Lygin, Infrakrasnye Spectry Adsorbirovannykh Soedineniy, Nauka, Moskow, 1972.
[19] K. Possemiers, P. van der Voort, E.F. Vansant, J. Chem. Soc., Faraday Trans. 92 (4) (1996) 679–684.
[20] V.A. Tertyh, A.A. Chuiko, V.A. Hranovskii, I.E. Neimark, J. Phys. Chem. (Russ.) 42 (7) (1968) 1758–1761.
[21] H.-P. Boehm, H. Knozinger, in: J.R. Anderson, M. Boudart (Eds.), Catalysis Science and Technology, vol. 4, Springer-Verlag, Berlin, Heidelberg, New York, 1983, pp. 39–209.
[22] J. Zechlin, B. Steinmetz, B. Tesche, G. Fink, Macromol. Chem. Phys. 201 (5) (2000) 515–524.
[23] K.-J. Chu, J.B. Soares, A. Pendilis, Macromol. Chem. Phys. 201 (2000) 552–557.
[24] N. Millot, A. Cox, C.C. Cantiti, Y. Molard, J.-M. Basset, Chem. Eur. J. 8 (2002) 1438–1442.
[25] N. Millot, C.C. Cantiti, A. Baudouin, J.-M. Basset, Chem. Comm. (2003) 2034–2035.